https://doi.org/10.5194/egusphere-2023-955
Preprint. Discussion started: 24 May 2023

Total Column Ozone Trends from the NASA Merged Ozone Time Series 1979 to 2021 Showing Limited Recovery to 1979 Amounts after Declining into the Mid 1990s

Jay Herman[1], Jerald Ziemke[2], and Richard McPeters[3]

[1]University of Maryland Baltimore County, Baltimore Maryland USA

[2]Morgan State University, Baltimore Maryland, USA

[3]NASA Goddard Space Flight Center, Greenbelt, Maryland, USA

Corresponding Author: Jay Herman Herman@umbc.edu

https://doi.org/10.5194/egusphere-2023-955
Preprint. Discussion started: 24 May 2023

Abstract

Monthly averaged total column ozone data Ω_{MOD} from the Merged Ozone Data set (MOD) were examined to show that the latitude-dependent ozone depletion turnaround dates $T_A(\theta)$ range from 1994 to 1998. Ω_{MOD} used in this study was created by combining data from Solar Backscattered Ultraviolet instruments (SBUV/SBUV-2) and the Ozone Mapping and Profiler Suite (OMPS-NP) from 1979 to 2021. $T_A(\theta)$ is defined as the date when the zonally average ozone ceased decreasing. The new calculated systematic latitude-dependent $T_A(\theta)$ shape should appear in atmospheric models that combine the effects of photochemistry and dynamics in their estimate of ozone recovery. Trends of zonally averaged total column ozone in percent per decade were computed before and after $T_A(\theta)$ using two different trend estimate methods that closely agree, Fourier Series Multivariate Linear Regression and linear regression on annual averages. During the period 1979 to $T_A(\theta)$ the most dramatic rates of SH ozone loss were P_D = -10.9 ± 3 % per decade at 77.5^{O}S and -8.5±0.9% per decade at 65^{O}S, which is about double the NH rate of loss of P_D = -5.6±4 %/decade at 77.5^{O}N and 4.4±1%/decade at 65^{O}N for the period 1979 to $T_A(\theta)$. After $T_A(\theta)$, there has been an increase at 65^{O}S of P_D = 1.6±1.4% per decade with smaller increases from 55^{O}S to 25^{O}S and a small decrease at 35^{O}N of -0.4±0.3 %/decade. Except for the Antarctic region, there only has been a small recovery in the Southern Hemisphere toward 1979 ozone values and almost none in the Northern Hemisphere.

https://doi.org/10.5194/egusphere-2023-955
Preprint. Discussion started: 24 May 2023

1.0 Introduction

Ozone is a photolytically produced, photochemically destroyed, and dynamically distributed atmospheric gas that plays a crucial role in protecting the planet from harmful ultraviolet (UV) radiation from the sun. The atmospheric presence of bromine and the release of chlorine from the UV dissociation of man-made chemicals, such as chlorofluorocarbons (CFCs), can break down the ozone layer. This is especially the case in the Antarctic region where heterogeneous chemistry on and within ice crystals in polar stratospheric clouds PSCs have a strong effect on the destruction of ozone during September and October (Solomon et al., 1986; 1999; 2016; Crutzen and Arnold, 1986; Khosrawi et al., 2011). As the sun rises in spring, chemically active nitrogen oxides, chlorine and bromine are released causing the ozone hole to develop within the region enclosed by the polar vortex winds. The weak levels of sunlight initiate and maintain the catalytic ozone loss photochemistry. In November and December, the isolating polar vortex winds break down and the Antarctic ozone hole region back fills from southern mid-latitudes. The recurring annual event triggered international action to limit the production and use of ozone-depleting substances (ODS) under the Montreal Protocol, which has been successful in reducing the emission of these substances, slowing down the depletion of the ozone layer globally, leading to a partial recovery in the Antarctic ozone hole region (Solomon et al., 2016; Strahan and Douglass 2018). After the mid-1990s, several studies have reported an increase in TCO, particularly in the mid to high latitudes of the Southern Hemisphere, as well as a reduction in the size and depth of the Antarctic ozone hole starting in the late 1990s (Solomon et al., 2016; Stone et al., 2018, Weber et al., 2022).

Ozone recovery was first observed in the mid-1990s when satellite data showed a stabilization and slight increase in ozone concentrations in the Antarctic ozone hole region. However, the recovery was not significant enough to be considered a trend at that time (Strahan and Douglass 2018). In the early 2000s, further analysis of satellite and ground-based data showed that the rate of ozone depletion had slowed down. After the mid-1990's, the cessation of ozone depletion has been most evident in the Southern Hemisphere SH polar region, where ozone depletion had been most severe, but the recovery has been slow or non-existent at other latitudes. Recently, Weber et al. (2022) reported positive statistically significant total column ozone (TCO) trends from 1996-2020 at southern middle and high latitudes, and over the SH polar cap in September. When dynamical terms were included in the regression, small positive trends were near the 2-standard deviation 2σ threshold at northern mid- and high-latitudes, with no trend detected in the tropics or over the NH polar cap.

Despite the success of the Montreal Protocol (Velders and Andersen, 2018), ozone concentrations continue to fluctuate, driven by natural and anthropogenic factors, such as changes in solar radiation, stratospheric circulation, global warming, and changing emissions of ozone precursors (Dameris and Baldwin, 2012; Weber et al., 2022). The discussion by Dameris and Baldwin (2012) explores possible effects of climate change on the dynamics of the atmosphere affecting ozone as ODSs change, and particularly the change in the Brewer-Dobson circulation (Brewer, 1949; Dobson et al., 1926) that transports ozone to mid- and high-latitudes.

https://doi.org/10.5194/egusphere-2023-955
Preprint. Discussion started: 24 May 2023

This study will calculate ozone trends based on new latitude dependent ozone recovery dates $T_A(\theta)$ ranging from 1994 (equatorial region and 60^{O}N to 70^{O}N) to 1998 (60^{O}S – 80^{O}S). Ozone data used in this study are a subset of the Merged Ozone Data MOD set (1970 – 2021) starting in 1979 with the Nimbus-7 SBUV (Solar Backscattered Ultraviolet) satellite instrument. From 1979 to 2021, the MOD data set was created by combining data from Solar Backscattered Ultraviolet instruments (SBUV/SBUV-2) and the Ozone Mapping and Profiler Suite (OMPS-NP). Methods of calculating trends from time series data are essential in the analysis of environmental and climate-related data. Here, we discuss two independent methods to estimate linear trends: 1) linear regression of annual averaged data and 2) Fourier time series decomposition or multivariate linear regression MLR (Ziemke et al., 2019). The two methods are compared and shown to give nearly identical results over their mutual latitude range of validity, 65^{O}S to 65^{O}N. The MLR method is not used in the regions poleward of the Arctic and Antarctic circles that have extended winter polar night.

1.1 The Merged Ozone Data Set MOD

Figure 1 (left panel) shows the MOD zonally averaged Ω_{MOD} TCO data (Frith et al., 2014; 2020) set as a function of latitude (5^O latitude bands from 77.5^{O}S to 77.5^{O}N) and time (January 1979 to December 2021). Part of the Antarctic ozone hole (75^{O}S to 80^{O}S) is shown (blue color), and the high latitude maxima, North and South, (red color), with low values in the equatorial region. Figure 1 (right panel) shows the 42-year zonal and time averaged ozone amounts and the maxima and minima annual envelopes as a function of latitude. Figure 1 shows the asymmetry in the monthly and zonally averaged ozone data between the hemispheres, with the Northern Hemisphere NH having more ozone than the Southern Hemisphere SH at corresponding latitudes. Part of the asymmetry is driven by the Spring Antarctic ozone hole backfilling in the SH summer.

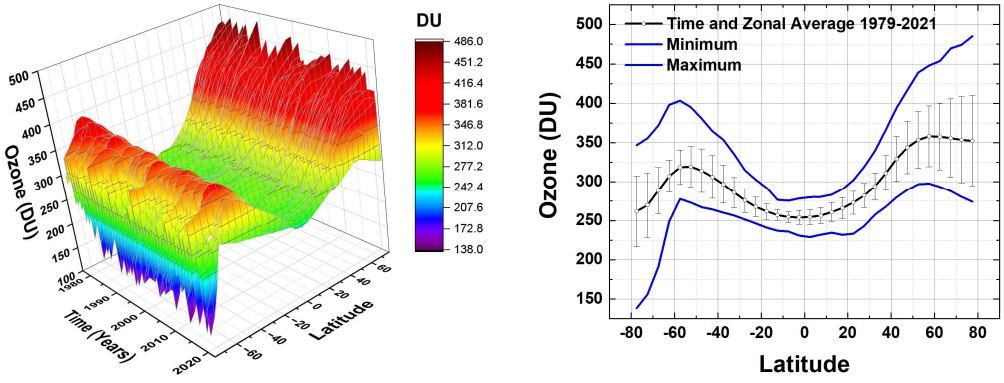

Fig. 1 Left: The zonally and monthly averaged Ω_{MOD} data set 1979 – 2021 and -77.5^O to 77.5^O. Right: Time and zonal averaged ozone and its maxima and minima 1979 – 2021. Error bars are 1 standard deviation ±1σ.

$\Omega_{MOD}(t,\theta)$ provides a global view of ozone levels needed to track changes in ozone concentrations over time t for each latitude band θ. The SBUV and OMPS-NP series of satellite instruments form the longest (1979 to 2022) continuous global ozone $\Omega_{MOD}(t,\theta)$ data record from a single instrument type. Merged

https://doi.org/10.5194/egusphere-2023-955
Preprint. Discussion started: 24 May 2023

ozone retrievals from the individual instruments use the version 8.7 retrieval algorithm (described by Weber et al., 2022) as an extension of the version 8.6 algorithm (Bhartia et al., 2013; McPeters et al., 2013; DeLand et al., 2012; Frith et al., 2017) specifically designed to improve cross calibrations between the later SBUV-type instruments in MOD starting from NOAA-16 in 2000. There were no external adjustments made to the ozone retrieval except for small high-altitude diurnal corrections to account for different measurement times between satellites and varying measurement time of day as individual satellite orbits slowly drift in equator crossing time. These adjustments are very minor in TCO (Frith, personal communication). Data from each instrument are selected based on quality criteria outlined in Frith et al. (2014; 2020) and then data are averaged during periods when more than one instrument was operational. The $\Omega_{MOD}(t,\theta)$ are available as a function of latitude and month, https://acd-ext.gsfc.nasa.gov/Data_services/merged/.

Analysis of the long-term ozone time series has been looked at extensively with references given in Weber et al., 2022. Methods for estimating trends from an oscillating time series with several distinct periodicities are well known (Ziemke et al., 2019; Stolarski et al. 1991;1992, Herman et al., 1993). For ozone, one of the difficulties in trend estimation is that the early part of the time series shows a strong ozone decrease at all latitudes that continued until the mid-1990s and then flattens out and shows almost no recovery thereafter toward 1979 values. The Ω_{MOD} time series has been used extensively in ozone assessments and State of the Climate reports and was recently compared to several other merged total ozone records in Weber et al., 2022. The validity of the Ω_{MOD} time series for estimating ozone trends was further checked (See Appendix Figs. A1 and A2) in this study by showing detailed comparisons between the deseasonalized Ω_{MOD} time series with the deseasonalized MLS (Microwave Limb Sounder) overlapping stratospheric ozone time series (2005 to 2023).

2.0 Trend Estimates from the MOD Ozone Data

Multivariate Linear Regression MLR is a Fourier based method for analyzing atmospheric time series data that decomposes the time series into its component parts, including trend, quasi-biennial oscillation QBO, solar cycle, ENSO (El Nino Southern Oscillation), seasonality, and noise resulting in a trend estimate and 2-standard deviation 2σ uncertainty estimates (Ziemke et al., 2019). Calculated 2σ uncertainties for the MLR trends included a first order autoregressive adjustment applied to the derived residuals (Weatherhead et al., 1998).

Linear trend estimates for the long-term changes in $\Omega_{MOD}(t, \theta_i)$ globally and as a function of latitude θ_i have been obtained using a generalized multivariate linear regression (MLR) model (e.g., Randel and Cobb, 1994, and references therein). Trends $B(\theta_i)$ were determined for $\Omega_{MOD}(t, \theta_i)$ using Eqns. 1 and 2.

$$\Omega_{MOD}(t, \theta_i) = A(\theta_i\, t) + B(\theta_i,t)\cdot t + C(\theta_i,t)\cdot QBO_1(t) + D(\theta_i,t)\cdot QBO_2(t) + E(\theta_i,t)\cdot ENSO(t) + F(\theta_i,t)\cdot Solar(t) + R(\theta_i, t) \quad (1)$$

where t is the month index (t=1 to 504 months with data for 1979–2021), $A(\theta_i\, t)$ is the seasonal cycle coefficient, $B(\theta_i,t)$ is the trend coefficient, $C(\theta_i,t)$ is the first empirical orthogonal function (EOF) QBO

https://doi.org/10.5194/egusphere-2023-955
Preprint. Discussion started: 24 May 2023

coefficient, $D(\theta_i,t)$ is the second EOF QBO coefficient, both representing the major components of the QBO variability, $E(\theta_i,t)$ is the ENSO coefficient, $F(\theta_i,t)$ is the solar cycle coefficient, and R(t) is the residual error time series. The F10.7 cm solar flux monthly time series is used for the Solar(t) proxy, first and second leading EOF QBO monthly time series proxies $QBO_1(t)$ and $QBO_2(t)$ are used for the QBO component (Wallace et al., 1993), and Nino 3.4 is used for ENSO(t). $A(\theta_i,t)$ involves 7 fixed constants while $B(\theta_i,t)$ (and all other remaining coefficients) involves 5 fixed constants for each θ_i. The harmonic expansion for A(t) (similar for the other coefficients) is (Eqn. 2)

$$A(t) = a(0) + \sum_{p=1}^{3}\left[a(p)\cos(2\pi pt/365) + b(p)\sin(2\pi pt/365)\right] \quad (2)$$

where a(p) and b(p) are constants. Statistical uncertainties for A(t) and $B(\theta_i)$ were derived from the calculated statistical covariance matrix involving the variances and cross-covariances of the constants (e.g., Guttman et al., 1982; Randel and Cobb, 1994). The linear deseasonalized trend results $B(\theta_i)$ are obtained for 14 latitude bands θ_i (centered on 65°S to 65°N). The latitudinal trends $P_D(\theta_i)$ are expressed in %/Decade given by Eq. 3, where the denominator D is either the time average of the area weighted global ozone average (Fig 3) or the time average $D(\theta_i) = <\Omega_{MOD}(t, \theta_i)>$ for each latitude band over the considered period. The whole year period considered is 1979 – 2021.

$$\mathbf{P_D(\theta_i) = 1000\ B(\theta_i)\ /D(\theta_i) \quad (\%\ /\ Decade)} \quad (3)$$

In the second method, the trend is estimated using annual integrals (annual averages) that remove the seasonality and other short-term oscillations but ignores longer term oscillations such as the 2-to-3-year QBO cycle and the 11-year solar cycle. A comparison of the two trend estimating methods is shown in Fig.2 for the entire 1979 to 2021 period showing that they agree quite closely, but that the annual average method has slightly larger two standard deviations 2σ than the MLR method.

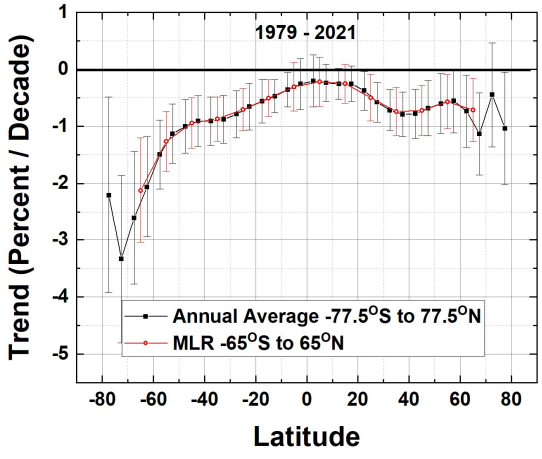

Fig. 2 The ozone trend $P_D(\theta)$ for the entire period 1979 – 2021 for two methods, MLR and Annual Average. The latitude grids for the two methods are offset to show the agreement in the trends and 2σ error bars.

https://doi.org/10.5194/egusphere-2023-955
Preprint. Discussion started: 24 May 2023

The Fig. 2 estimation of linear long-term trends since 1979 is misleading, since ozone showed significant annual declines until the mid-1990s and then increased slightly thereafter, meaning the average long-term time series is non-linear. The usual procedure is to determine linear trends separately before and after the turnaround dates T_A (Zhang and Thompson, 2021; Weber et al., 2022). However, as is shown later, there is no single turnaround date applicable to all the latitudes between 80^{O}S and 80^{O}N. Instead, there is a range spanning 1994 to 1998.

In this study the Locally Weighted Scatterplot Smoothing Lowess(f) technique is used to find the turn-around dates (Figs. 3 and 4), where f = the fraction of data averaged together (Cleveland, 1979 and Cleveland and Devlin, 1988).

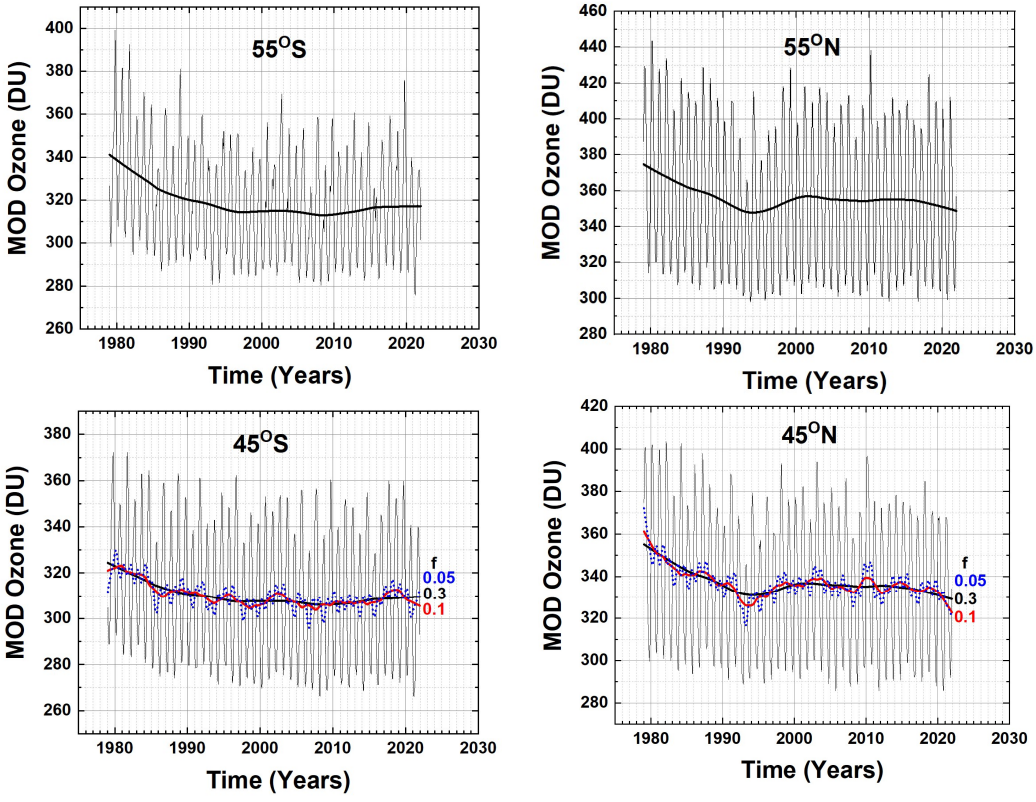

Fig. 3 Ω_{MOD} in four latitude bands and Lowess(0.3) fitting functions (f = 0.3, black lines). Examples of different f = 0.1 (Red) and 0.05 (blue dots) are shown at 45^{O}S and 45^{O}N. Note the slight downturn in the Lowess(0.3) at 45^{O}N and 55^{O}N.

Figure 3 shows the Lowess(0.3) fits (black curves) to the Ω_{MOD} data for four sample latitude bands 55^{O}S, 45^{O}S, 55^{O}N, and 45^{O}N that tracks the longer-term changes in the Ω_{MOD} time series. Also shown for 45^{O}N and 45^{O}S are examples of f = 0.1 (red) and f = 0.05 (blue dots). The values of T_A for f = 0.1 and 0.05 are approximately the same but are harder to see. The Lowess(0.3) degree of smoothing removes all short-term effects on ozone such as volcanic eruptions from El Chichon (1982) and Mt. Pinatubo (1991), both

https://doi.org/10.5194/egusphere-2023-955
Preprint. Discussion started: 24 May 2023

well before the earliest estimated turnaround time T_A in 1994. The Lowess(0.05) fit (blue dots) shows considerable structure with a minimum in 1993 that is likely related to the Mt. Pinatubo eruption and a modest El Nino effect in 1991-1992. In the equatorial zone at 5^OS and 5^ON, there are two minima, f=0.05, occurring in 1992 and 1994.

Figure 4 shows the Lowess(0.3) fits to the Ω_{MOD} data (1979 to 2021) for 16 latitude bands, $-75^O < \theta < 75^O$ on an expanded ozone scale. Each of the Lowess(0.3) plots for the various latitudes shows different periods of ozone decrease and subsequent turnaround $T_A(\theta)$ after the mid-1990's. Use of expanded ozone scales appear to show a sharp downturn at some latitudes (25^ON to 75^ON). As shown later, the apparent downturn in the Lowess(0.3) fit to Ω_{MOD} after 2010 is not yet statistically significant as an indicator of long-term decrease.

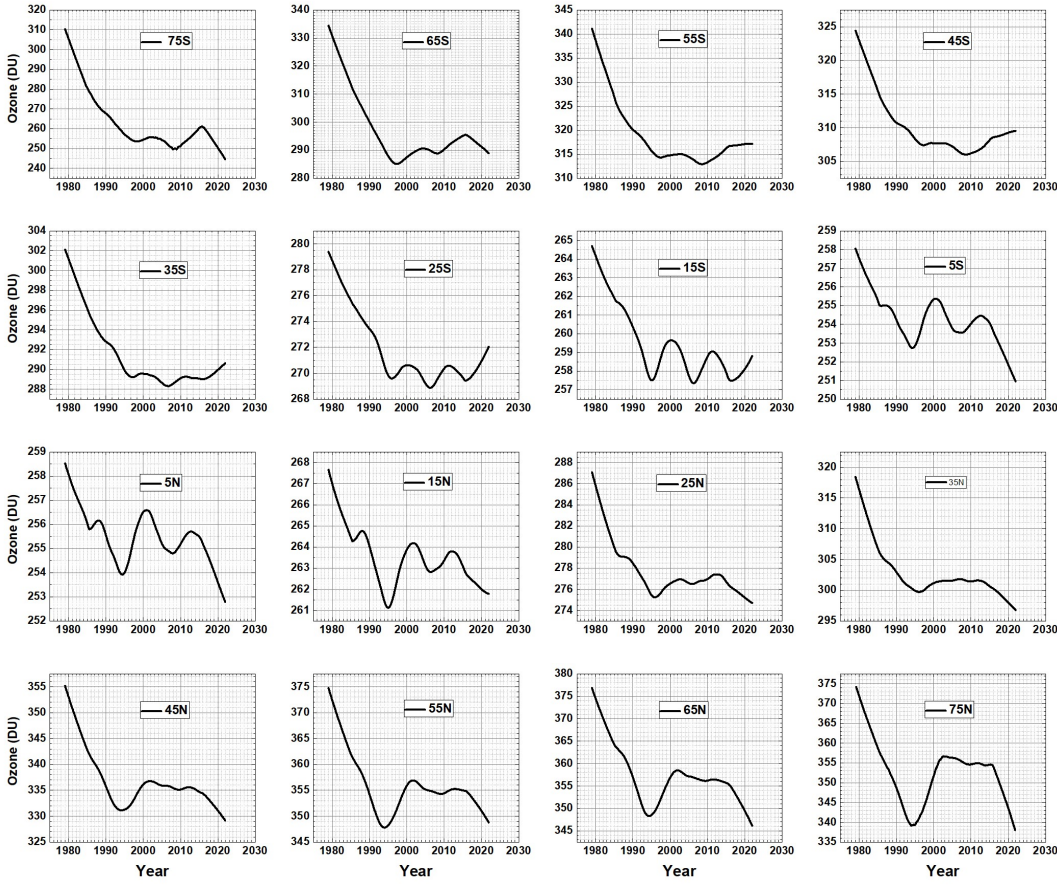

Fig. 4 Lowess(0.3) fits to the Ω_{MOD} data for 16 latitude bands Used to determine the turnaround dates.

Figure 5 shows the turnaround dates $T_A(\theta)$ that are obtained by taking the 1st derivative and finding the zero-crossing time corresponding to the appropriate minimum value in Fig. 4. The exact turnaround

https://doi.org/10.5194/egusphere-2023-955
Preprint. Discussion started: 24 May 2023

dates determined have a precision of ±0.1 years. The uncertainty does not affect the calculation of trends before and after the estimated $T_A(\theta)$. What is interesting is that some of the turnaround dates in Fig. 5 are separated by over 4 years. Figure 5 shows a near symmetry for early turnaround dates 1994-1996 for low latitudes between ±25^O that corresponds to the Brewer-Dobson ozone upwelling region (Brewer et al., 1926; Dobson, 1949; Butchart, 2014) where most of the ozone is created by sunlight and then transported poleward. At poleward latitudes, the turnaround dates are quite different, with a delayed date, 1997, at high SH latitudes (45^{O}S – 65^{O}S), 1998 at 75^{O}S, and 1994 at high NH latitudes (45^{O}N to 75^{O}N). The SH delay to 1997 is caused by the presence of the Spring Antarctic Ozone Hole and backfilling during the summer months after the polar vortex winds break down in October - November.

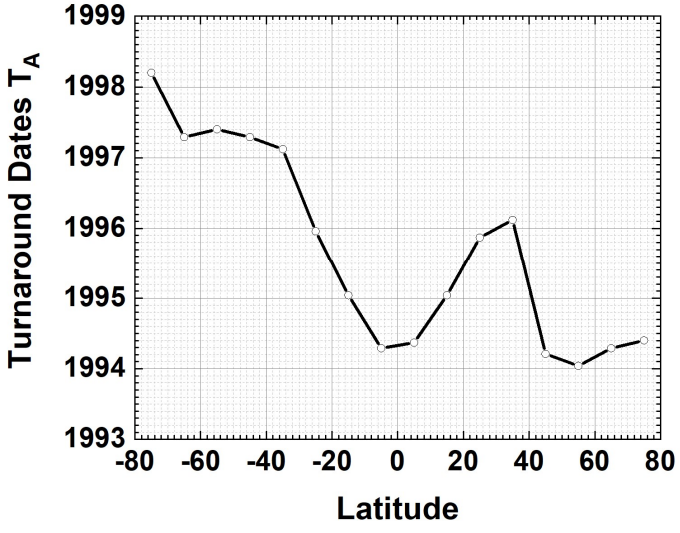

Fig 5 Turnaround dates $T_A(\theta)$ as a function of latitude from Fig.4

Table 1 Turnaround Dates $T_A(\theta)$

Latitude	T_A	Latitude	T_A
-75	1998.20	5	1994.37
-65	1997.29	15	1995.04
-55	1997.46	25	1995.87
-45	1997.29	35	1996.12
-35	1997.12	45	1994.21
-25	1995.96	55	1994.04
-15	1995.04	65	1994.29
-5	1994.29	75	1994.40

The general $T_A(\theta)$ pattern shown in Fig. 5 should appear in model calculations as a signature of the combined effects of photochemistry and dynamics on the cessation of decreasing ozone in the mid-1990s.

https://doi.org/10.5194/egusphere-2023-955
Preprint. Discussion started: 24 May 2023

Trends (linear slopes) $P_D(\theta)$ in percent per decade are estimated (Eqn. 3) for the separate periods before and after $T_A(\theta)$ in each latitude band (Fig. 6) and for the entire period (Fig. 2). The linear slopes obtained by the two methods, MLR and annual average closely agree (Figs. 2 and 6). Table 2 contains the data from Figs. 6a and 6b.

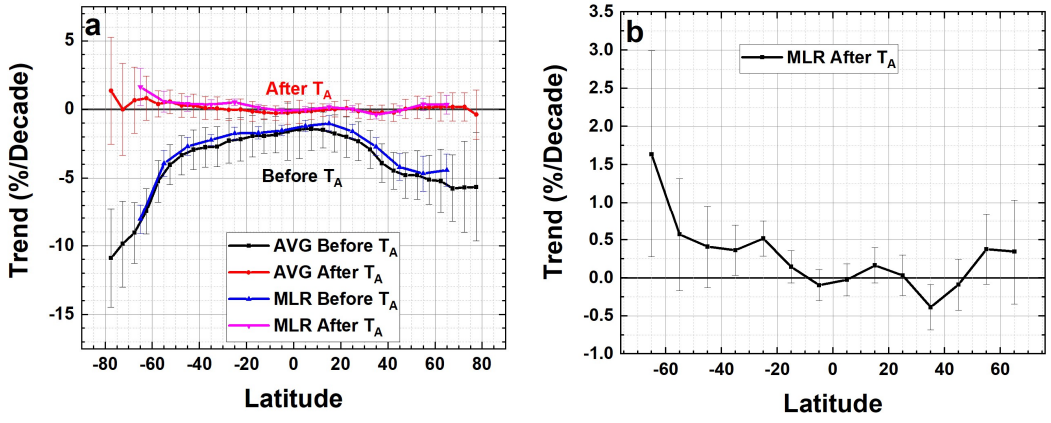

Fig. 6a Ozone trends $P_D(\theta)$ (percent per decade) using the MLR and Annual Average methods before and after the turn-around times $T_A(\theta)$ in Fig. 5. 6b A magnified version of the MLR estimated trends after T_A with 2σ uncertainties.

Table 2 MLR Trends (%/decade) ± 2σ

Latitude	P_D Before T_A	P_D After T_A
-65	-8.04±1.1	1.64±1.4
-55	-3.93±1.0	0.57±0.7
-45	-2.69±0.7	0.41±0.5
-35	-2.22±0.4	0.36±0.3
-25	-1.75±0.5	0.52±0.2
-15	-1.71±0.4	0.15±0.2
-5	-1.54±0.4	-0.10±0.2
5	-1.21±0.4	-0.03±0.2
15	-1.01±0.6	0.16±0.2
25	-1.61±0.5	0.03±0.3
35	-2.71±0.6	-0.39±0.3
45	-4.20±1.0	-0.09±0.3
55	-4.67±1.3	0.38±0.5
65	-4.43±1.2	0.35±0.7

The latitude dependent trends derived by Weber et al., 2022 (their Fig. 3) agree closely with the trends shown in Fig. 6 with Weber et al. using 1996.5 as the approximate T_A for all latitudes but does suggest T_A = 2000 for the polar regions. As mentioned earlier, the trend estimates are not very sensitive to the exact T_A, but the shape of $T_A(\theta)$ should be a marker contained in model calculations.

https://doi.org/10.5194/egusphere-2023-955
Preprint. Discussion started: 24 May 2023

Because of the severity of the Antarctic ozone hole ozone before T_A, total column ozone decreased at a rate of P_D= -10.9±3.6% at 77.5^{O}S and -8.0±1.1% per decade at 65^{O}S, near the edge of the nearly continuous Spring polar vortex wind, during the period from 1979 to 1997 with smaller decreases at 55^{O}S to 25^{O}S. The seasonal breakup of the Antarctic polar vortex winds led to an inflow of ozone from other SH latitudes contributing to depletion in most of the SH. In the NH the decreases were smaller before T_A because of the absence of continuous polar vortex winds and an Arctic ozone hole. At 77.5^{O}N was P_D = -5.6±4%/decade and at 65^{O}N P_D = -4.4±0.35 %/decade After the turnaround period T_A, ozone at 65^{O}S increased at P_D = 1.6±1.4%/decade based on the MLR method. After T_A, most other latitudes (Fig. 6b) show stationary ozone amounts within 2σ.

The Lowess(0.3) plots in Fig. 4 suggest that Ω_{MOD} has been declining since approximately 2010 from 5^{O}S to 65^{O}N but still increasing from 45^{O}S to 65^{O}S (Fig. 7). However, computing the trends from either the MLR or annual average methods suggest a small decline from 15^{O}S to 65^{O}N of 1.5 ± 2% per decade that is not significant at the 2σ level.

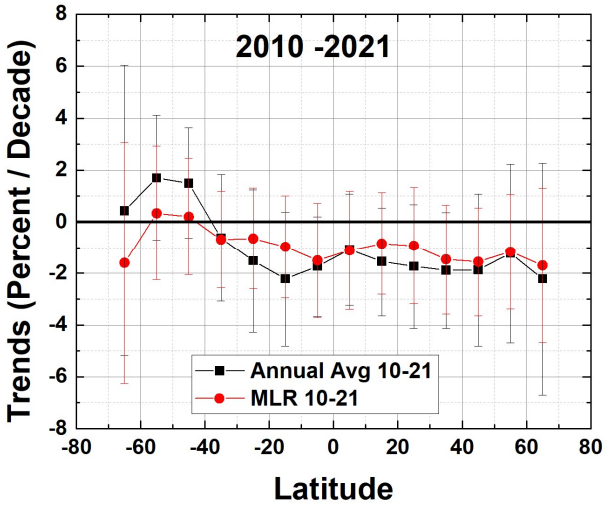

Fig. 7 Ozone trends $P_D(\theta)$ (Percent per Decade) for the period 2010 – 2022 for the Annual Average and MLR methods.

A comparison of deseasonalized $\Omega_{MOD}(t,\theta)$ with deseasonalized Microwave Limb Sounder MLS (see Appendix Figs. A1, A2, and A3) Stratospheric Ozone from 2005 to 2021 shows small average (Lowess(0.3)) differences that are not statistically significant. For 2016 to 2018, Ω_{MOD} is obtained from NOAA-19 SBUV plus OMPS-NP and from OMPS-NP since 2018. The largest Lowess (0.3) differences, deseasonalized Ω_{MOD} – deseasonalized MLS, since 2016 are at 65^{O}S of -4±9 DU, 5^{O}S of -1±2 DU, 65^{O}N of -2.5±7DU, 35^{O}N of -1±2.6 DU, 25^{O}N of -0.5±2 DU, 15^{O}N of -0.5±2DU, and 5^{O}N of -1±2 DU. Other latitudes

https://doi.org/10.5194/egusphere-2023-955
Preprint. Discussion started: 24 May 2023

55^{O}S to 15^{O}S and 55^{O}N have no difference or are slightly positive. This suggests that the calibrations of the later SBUV-2 and OMPS-NP instruments are stable.

3.0 Summary

The monthly averaged Merged Ozone Data set Ω_{MOD} (5^{O} latitude bands, 77.5^{O}S to 77.5^{O}N) from 1979 to 2021 were also averaged into 10^{O} latitude bands 75^{O}S < θ < 75^{O}N. A smoothed Ω_{MOD} version based on Lowess(0.3) was used to determine the approximate dates of the latitude dependent ozone turnaround $T_A(\theta)$ ranging from 1994 to 1998. The systematic latitude dependent pattern $T_A(\theta)$ should appear in atmospheric models that combine the effects of photochemistry and dynamics in their estimate of ozone recovery. Trends of ozone $P_D(\theta)$ in percent per decade were computed before and after the latitude dependent $T_A(\theta)$ using two different methods, MLR and annual averages, that closely agree over their mutual latitude range of validity, 65^{O}S to 65^{O}N. The most dramatic rates of ozone loss were P_D = -10.9±3.6% decade at 77.5^{O}S and -8.0±1.1%/decade at 65^{O}S, which is about double the rate of loss of P_D = -5.7±4 %/decade at 77.5^{O}N and -4.4±1.2% per decade at 65^{O}N. During the period after the start of recovery T_A to 2021, there has been a small increase at latitudes in the SH from 25^{O}S to 65^{O}S with the largest value being 1.6±1.4% per decade at 65^{O}S. Aside from the small increases in the SH region there has been no statistically significant ozone recovery toward 1979 values, just an almost constant ozone amount after $T_A(\theta)$. During the period 2010 to 2021, there has been a small apparent decrease in ozone amount in Ω_{MOD} that is not statistically significant at the 2-standard deviation level. A comparison between Ω_{MOD} and MLS stratospheric column ozone shows some small differences both positive and negative after 2016 when the Lowess (0.3) smoothing of the total ozone shows the largest decrease.

https://doi.org/10.5194/egusphere-2023-955
Preprint. Discussion started: 24 May 2023

Appendix

The MOD TCO data record since 2018 is obtained from OMPS-NP, which appears to show decreasing TCO (Fig. 4). Because of this, the deseasonalized Ω_{MOD} are compared with MLS (Microwave Limb Sounder) deseasonalized stratospheric column ozone for the period 2004 to 2021 to look for calibration drifts in the Ω_{MOD} time series. The question addressed here is not the absolute agreement between Ω_{MOD} and the MLS mostly stratospheric ozone column, but rather if there is a systematic drift between the two data sets after 2016. Figures A1 and A2 show that the difference between the two deseasonalized time series for latitudes from 65^{O}S to 65^{O}N and for the entire period 2005 – 2021. Of interest is the period 2016 to 2021 when Ω_{MOD} was derived using NOAA-19 SBUV plus OMPS-NP 2016 – 2018 and from OMPS-NP since 2018.

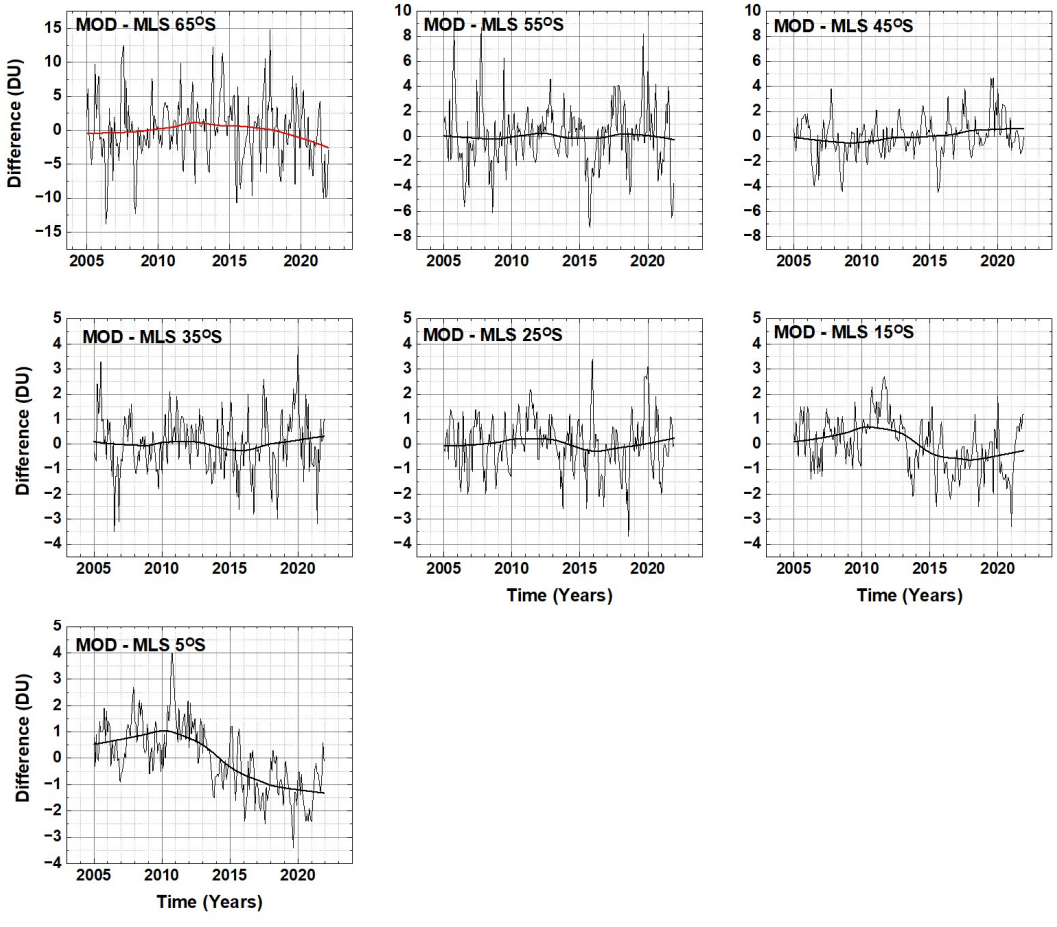

Fig. A1 A comparison of deseasonalized Ω_{MOD} with deseasonalized MLS stratospheric column ozone for 65^{O}S to 5^{O}S.

https://doi.org/10.5194/egusphere-2023-955
Preprint. Discussion started: 24 May 2023

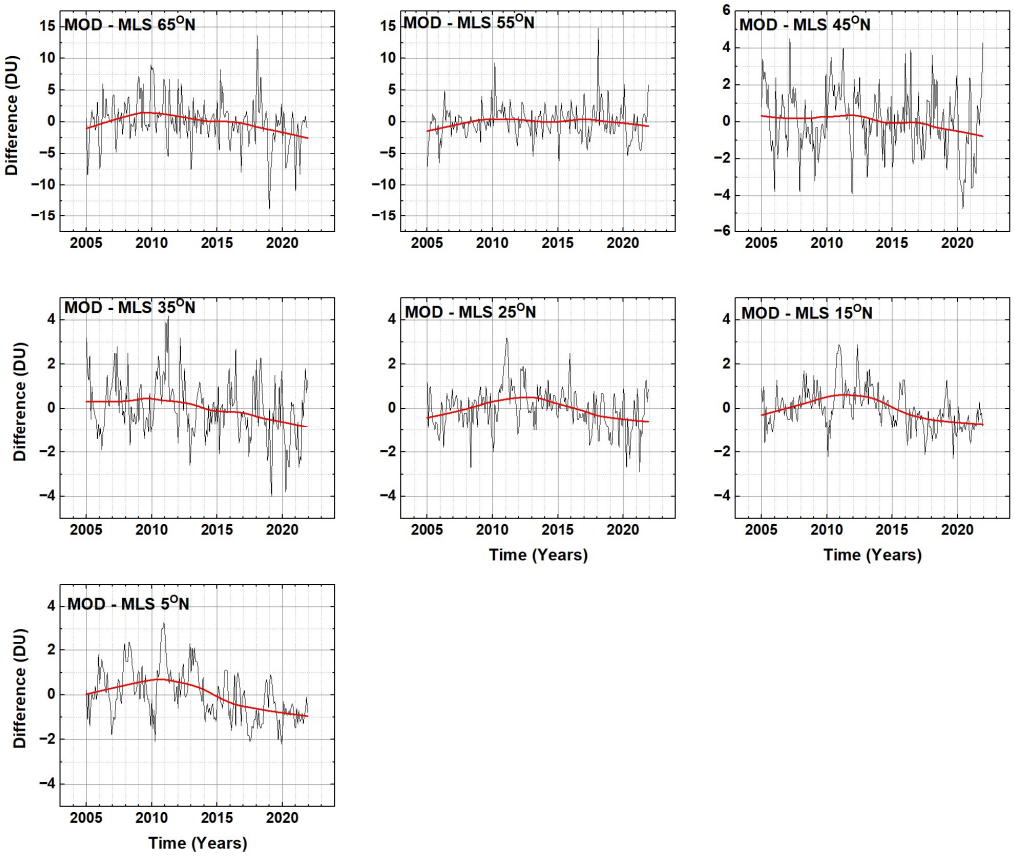

Fig. A2 A comparison of deseasonalized MOD total ozone with deseasonalized MLS stratospheric column ozone for 5°N to 65°N. Variations of ±3DU are within the MOD merged record uncertainties.

The differences in Figs A1 and A2 between Ω_{MOD} and MLS since 2016 are not statistically significant at the 2σ level. Variations of ± 3DU are within the Ω_{MOD} merged record uncertainties.

The differences in 2021 average of Lowess(0.3) are summarized in Fig. A3 along with the 2σ standard deviations estimated from the average of the deseasonalized time series. One latitude shows a statistically significantly difference, 5°N. The conclusion is that there is no statistically significant drift between Ω_{MOD} and MLS stratospheric ozone.

https://doi.org/10.5194/egusphere-2023-955
Preprint. Discussion started: 24 May 2023

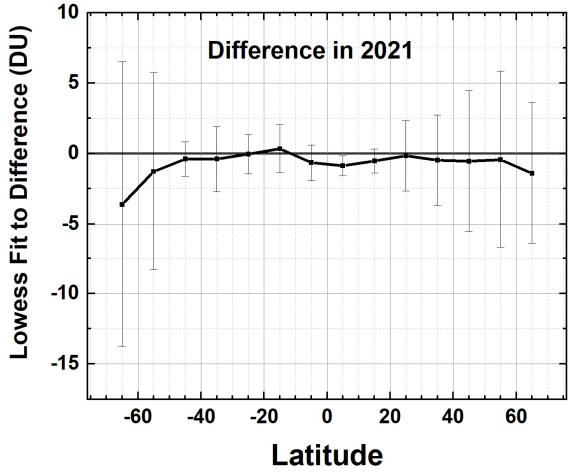

Fig. A3 The difference between the 2021 average Lowess (0.3) fit to Ω_{MOD} – MLS O_3 during 2021. The 2σ standard deviations are estimated from the average of the deseasonalized time series during 2021 shown in Figs. A1 and A2.

273

274

https://doi.org/10.5194/egusphere-2023-955
Preprint. Discussion started: 24 May 2023

4.0 References

Bai, K., N.-B. Chang, R. Shi, H. Yu, and W. Gao, An intercomparison of multidecadal observational and reanalysis data sets for global total ozone trends and variability analysis, J. Geophys. Res. Atmos., 122, 7119–7139, doi:10.1002/2016JD025835, 2017.

Bhartia, P. K. , R. D. McPeters, L. E. Flynn, S. Taylor, N. A. Kramarova, S. Frith, B. Fisher, and M. DeLand, Solar Backscatter UV (SBUV) total ozone and profile algorithm. Atmos. Meas. Tech., 6, 2533–2548, doi:10.5194/amt-6-2533-2013, 2013.

Brewer, A. W., Evidence for a world circulation provided by the measurements of helium and water vapour distribution in the stratosphere, Quarterly Journal of the Royal Meteorological Society. 75 (326): 351–363. Bibcode:1949QJRMS..75..351B. doi:10.1002/qj.49707532603. ISSN 1477-870X, 1949.

Crutzen, P. J. and Arnold, F.: Nitric acid cloud formation in the cold Antarctic stratosphere: a major cause for the springtime “ozone hole”, Nature, 342, 651–655, 1986.

Dameris, Martin and Mark P. Baldwin, Impact of Climate Change on the Stratospheric Ozone Layer, Stratospheric Ozone Depletion and Climate Change, Edited by Rolf Muller, Chapter 8, 214-252, Royal Society of Chemistry 2012.

Dobson, G. M. B.; Harrison, D. N.; Lindemann, F. A., Measurements of the amount of ozone in the Earth's atmosphere and its relation to other geophysical conditions, Proceedings of the Royal Society of London. Series A, Containing Papers of a Mathematical and Physical Character. 110 (756): 660–693. Bibcode:1926RSPSA.110..660D. doi:10.1098/rspa.1926.0040. 1926.

Butchart, N., The Brewer-Dobson circulation, Rev. Geophys.,52, 157–184, doi:10.1002/2013RG000448, 2014.

Cleveland, W.S., Robust Locally Weighted Regression and Smoothing Scatterplots, Journal of the American Statistical Association, Vol. 74, pp. 829-836, 1979.

Cleveland, W.S. and Devlin, S.J., Locally Weighted Regression: An Approach to Regression Analysis by Local Fitting," Journal of the American Statistical Association, Vol. 83, pp. 596-610, 1988.

DeLand, M. T., S. L. Taylor, L. K.Huang, and B. L. Fisher, Calibration of the SBUV version 8.6 ozone data product, Atmos. Meas. Tech., 5, 2951–2967, doi:10.5194/amt-5-2951-2012, 2012.

Frith, S. M., N. A. Kramarova, R. S. Stolarski, R. D. McPeters, P. K. Bhartia, and G. J. Labow, Recent changes in total column ozone based on the SBUV Version 8.6 Merged Ozone Data Set, J. Geophys. Res. Atmos., 119, 9735-9751, doi:10.1002/2014JD021889, 2014.

Frith, S. M., Stolarski, R. S., Kramarova, N. A., and McPeters, R. D.: Estimating uncertainties in the SBUV Version 8.6 merged profile ozone data set, Atmos. Chem. Phys., 17, 14695–14707, https://doi.org/10.5194/acp-17-14695-2017, 2017.

https://doi.org/10.5194/egusphere-2023-955
Preprint. Discussion started: 24 May 2023

311 Frith, S. M., Bhartia, P. K., Oman, L. D., Kramarova, N. A., McPeters, R. D., and Labow, G. J.: Model-based
312 climatology of diurnal variability in stratospheric ozone as a data analysis tool, Atmos. Meas. Tech., 13,
313 2733-2749, https://doi.org/10.5194/amt-13-2733-2020, 2020.
314
315 Guttman, I., Linear Models, An Introduction, 358 pp., Wiley-Interscience, New York, 1982.

316 Herman, J.R., R. McPeters, D. Larko, Ozone depletion at northern and southern latitudes derived from
317 January 1979 to December 1991 Total Ozone Mapping Spectrometer data, 98, 13783-12793
318 https://doi.org/10.1029/93JD00601, 1993.

319 Khosrawi, F., Urban, J., Pitts, M. C., Voelger, P., Achtert, P., Kaphlanov, M., Santee, M. L., Manney, G. L.,
320 Murtagh, D., and Fricke, K.-H.: Denitrification and polar stratospheric cloud formation during the Arctic
321 winter 2009/2010, Atmos. Chem. Phys., 11, 8471–8487, https://doi.org/10.5194/acp-11-8471-2011,
322 2011.

323 McPeters, R. D., P. K. Bhartia, D. Haffner, G. J. Labow, and L. Flynn, The version 8.6 SBUV ozone data
324 record: An overview, J. Geophys. Res. Atmos., 118, 8032-8039, doi:10.1002/jgrd.50597., 2013.

325 Randel, W. J., and J. B. Cobb, Coherent variations of monthly mean total ozone and lower stratospheric
326 temperature, J. Geophys. Res., 99, 5433--5447, 1994.

327 Solomon, S., Garcia, R. R., Rowland, F. S., and Wuebbles, D. J.: On the depletion of Antarctic ozone,
328 Nature, 321, 755–758, 1986.

329 Solomon, S., Stratospheric ozone depletion: a review of concepts and history, Rev. Geophys., 37, 275–
330 316, 1999.

331 Solomon, Susan, Diane J. Ivy, Doug Kinnison, Michael J. Mills, Ryan R. Neely, Iii, And Anja Schmidt,
332 Emergence of healing in the Antarctic ozone layer, Vol 353, 269-274 DOI: 10.1126/science.aae0061,
333 2016.

334 Stolarski R. D., P. Bloomfield, R. D. McPeters, and J. R. Herman, Total ozone trends deduced from
335 Nimbus 7 TOMS data, Geophys., Res., Lett., 18, https://doi.org/10.1029/91GL01302, 1991.

336 Stolarski R, Bojkov R, Bishop L, Zerefos C, Staehelin J, Zawodny J. Measured trends in stratospheric
337 ozone, Science, Apr 17;256(5055):342-9. doi: 10.1126/science.256.5055.342. PMID: 17743110, 1992.
338
339 Stone, K. A., Solomon, S., and Kinnison, D. E., On the identification of ozone recovery. Geophysical
340 Research Letters, 45, https://doi.org/10.1029/2018GL077955, 2018.
341
342 Strahan, S. E., and Douglass, A. R., Decline in Antarctic ozone depletion and lower stratospheric chlorine
343 determined from Aura Microwave Limb Sounder observations. Geophysical Research Letters, 45, 382–
344 390. https://doi.org/10.1002/2017GL074830, 2018.

345 Velders, G. J., & Andersen, S. O. (2018). The Montreal Protocol on Substances that Deplete the Ozone
346 Layer and its amendments: An overview. Air Pollution and Health, 11-28, 2018.

https://doi.org/10.5194/egusphere-2023-955
Preprint. Discussion started: 24 May 2023

Wallace, J. M., R. L. Panetta, and J. Estberg, Representation of the equatorial stratospheric quasi-biennial oscillation in EOF phase space, J. Atmos. Sci., 50, 1751--1762, https://doi.org/10.1175/1520-0469(1993)050<1751:ROTESQ>2.0.CO;2, 1993.

Weatherhead, E. C., Reinsel, G. C., Tiao, G. C., Meng, X.-L., Choi, D., Cheang, W.-K., Keller, T., DeLuisi, J., Wuebbles, D. J., Kerr, J. B., Miller, A. J., Oltmans, S. J., and Frederick, J. E.: Factors affecting the detection of trends: Statistical considerations and applications to environmental data, 103,17149–17161, https://doi.org/10.1029/98JD00995, 1998.

Weber, Mark, Carlo Arosio, Melanie Coldewey-Egbers, Vitali E. Fioletov, Stacey M. Frith, Jeannette D. Wild, Kleareti Tourpali, John P. Burrows, and Diego Loyola, Global total ozone recovery trends attributed to ozone-depleting substance (ODS) changes derived from five merged ozone datasets, https://doi.org/10.5194/acp-22-6843-2022, ACP, 22, 6843–6859, 2022

Zhang, L., & Thompson, A. M. (2021). Ozone depletion and recovery: A review of the history and current state of research. Environmental Pollution, 287, 117605, 2021.

Ziemke, Jerry R. Luke D. Oman, Sarah A. Strode, Anne R. Douglass, Mark A. Olsen, Richard D. McPeters, Pawan K. Bhartia, Lucien Froidevaux, Gordon J. Labow, Jacquie C. Witte, Anne M. Thompson, David P. Haffner, Natalya A. Kramarova, Stacey M. Frith, Liang-Kang Huang, Glen R. Jaross, Colin J. Seftor, Mathew T. Deland, Steven L. Taylor, Trends in global tropospheric ozone inferred from a composite record of TOMS/OMI/MLS/OMPS satellite measurements and the MERRA-2 GMI simulation, Atmospheric Chemistry and Physics, 10.5194/acp-19-3257-2019, **19**, 5, (3257-3269), 2019.

Author contribution:

Jay Herman is responsible for writing the text, the annual integral trend calculations, and all the figures. Jerald Ziemke supplied the MLR trend calculations and the comparison with MLS. Richard McPeters supplied the MOD ozone as a continuous function of time from 1979 to 2021 for each latitude band.

Data Availability

The original data used are publicly available in an ASCII format**.**
https://acd-ext.gsfc.nasa.gov/Data_services/merged/
and processed data in Excel format
https://avdc.gsfc.nasa.gov/pub/DSCOVR/JayHerman/MOD_Ozone_Trends/

Competing interests:

The authors declare that they have no conflict of interest.

https://doi.org/10.5194/egusphere-2023-955
Preprint. Discussion started: 24 May 2023

Acknowledgements:
The authors want to acknowledge the contribution and help of Stacey Frith for compiling the SBUV and OMPS-NP data sets to produce the long ozone data record. She also reviewed the paper and added some important corrections.

Figure Captions

Fig. 1 Left: The zonally and monthly averaged Ω_{MOD} data set 1979 – 2021 and -77.5^{O} to 77.5^{O}. Right: Time and zonal averaged ozone and its maxima and minima 1979 – 2021. Error bars are 1 standard deviation $\pm 1\sigma$.

Fig. 2 The ozone trend $P_D(\theta)$ for the entire period 1979 – 2021 for two methods, MLR and Annual Average. The latitude grids for the two methods are offset to show the agreement in the trends and 2σ error bars.

Fig. 3 Ω_{MOD} in four latitude bands and Lowess(0.3) fitting functions (f = 0.3, black lines). Examples of different f = 0.1 (Red) and 0.05 (blue dots) are shown at 45^{O}S and 45^{O}N. Note the slight downturn in the Lowess(0.3) at 45^{O}N and 55^{O}N.

Fig. 4 Lowess(0.3) fits to the Ω_{MOD} data for 16 latitude bands Used to determine the turnaround dates.

Fig 5 Turnaround dates $T_A(\theta)$ as a function of latitude from Fig.4

Fig. 6a Ozone trends $P_D(\theta)$ (percent per decade) using the MLR and Annual Average methods before and after the turn-around times $T_A(\theta)$ in Fig. 3. 6b. A magnified version of the MLR estimated trends after T_A with 2σ uncertainties.

Fig. 7 Ozone trends $P_D(\theta)$ (Percent per Decade) for the period 2010 – 2022 for the Annual Average and MLR methods.